Complex scaling in NLEFT & NLEFT calculations of proton-rich nuclei

Shuang Zhang

Nuclear Lattice EFT Collaboration

Contents

Complex scaling in NLEFT

- **Complex scaling method**
- **1D 1-body**
- **3D 2-body**

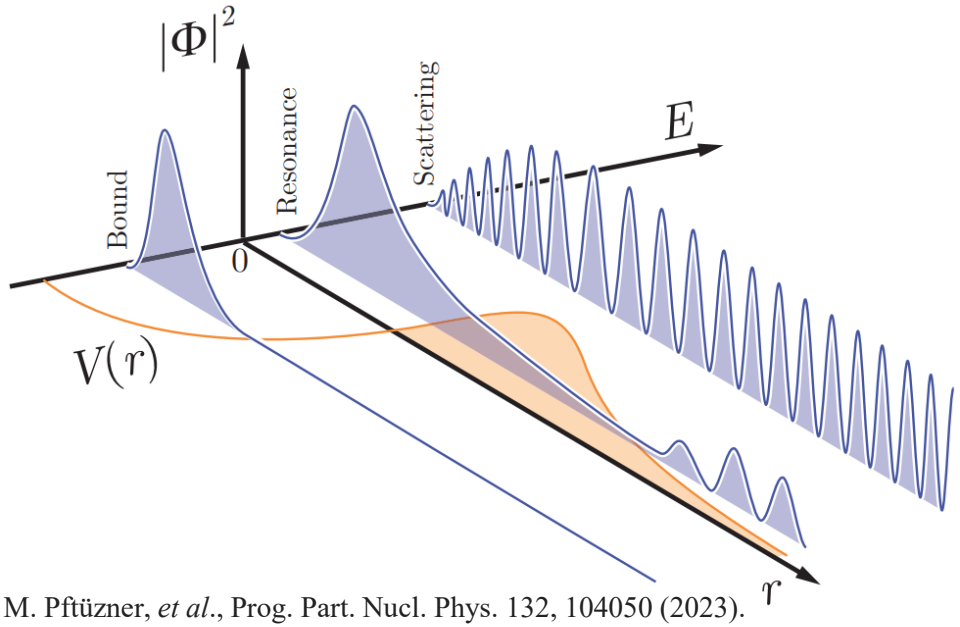

M. Pftüzner, *et al*., Prog. Part. Nucl. Phys. 132, 104050 (2023).

Complex scaling method

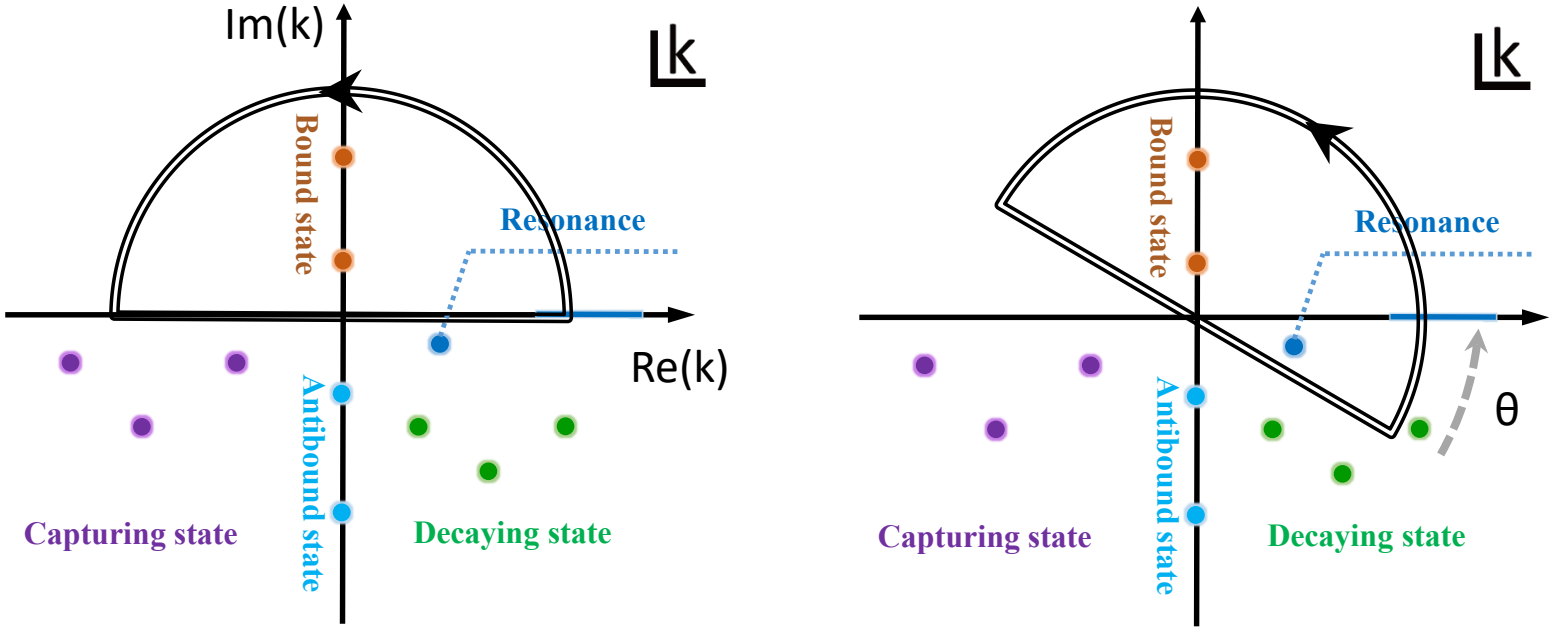

Transformation operator: $U(\theta)r = re^{i\theta}, U(\theta)k = ke^{-i\theta}$

$$H(\theta) = U(\theta)HU^{-1}(\theta)$$

where $U^{-1}(\theta) = U(-\theta)$.

Then $H\Psi = E\Psi$ can be written as

$$H(\theta)\Psi(\theta) = E(\theta)\Psi(\theta)$$

with $\Psi(\theta) = U(\theta)\Psi = e^{i3f\theta/2}\Psi(re^{i\theta})$

Complex scaling method

ABC theorem:

I. The bound states of H and H(θ) are the same;

II. The spectrum of the H is rotated down by an angle θ into the complex-energy plane, exposing a higher Riemann sheet of the resolvent;

III. The resonant states of H are also eigenvalues of H(θ) and their wavefunctions are square integrable;

Aguilar, J., Combes, J.M. A, Commun.Math. Phys. 22, 269–279 (1971).
Balslev, E., Combes, Commun.Math. Phys. 22, 280–294 (1971)

Bi-orthogonal basis & c-products:

Non-Hermitian Hamiltonian:

$$\tilde{\Psi}^{\theta}(k) = \Psi^{\theta}(-k^{*})$$

Scalar product is defined as

$$\langle \Psi^{\theta} | \Psi^{\theta} \rangle = \langle \Psi^{\theta}(k,r) | \Psi^{\theta}(k,r) \rangle = \int dr \tilde{\Psi}^{\theta}(k,r)^{*} \Psi^{\theta}(k,r) = \int dr \Psi^{\theta}(-k^{*},r)^{*} \Psi^{\theta}(k,r)$$

$$= \int dr \Psi^{\theta}(-k,r) \Psi^{\theta}(k,r) = \int dr \Psi^{\theta}(E,r) \Psi^{\theta}(E,r)$$

Complex scaling method

For the case of a central potential:

$$\frac{\hbar^2}{2\mu}[-\frac{d^2}{dr^2}+\frac{l(l+1)}{r^2}]e^{-2i\theta}+V(re^{i\theta})\Psi_l^\theta(k,r)=E(\theta)\Psi_l^\theta(k,r)$$

The asymptotic behavior at $r\to\infty$:

$$\Psi_l^\theta(k,r)\to[f_l^{+\theta}(k)e^{-ikre^{i\theta}}-(-1)^l f_l^{-\theta}(k)e^{ikre^{i\theta}}]$$

Here $f_l^{+\theta}(k), f_l^{-\theta}$ are Hankel functions.

The wave functions of bound states ($k = ik_p$, $k_p > 0$) maintain the damping behavior.

For resonant states $k = k_r - ik_i$, k_r, $k_i > 0$:

$$\begin{aligned}e^{ikre^{i\theta}} &= e^{i(k_r-ik_i)r(cos\theta+isin\theta)}\\ &= e^{(-k_r sin\theta+k_i cos\theta)r}e^{ik_r(cos\theta+k_i sin\theta)}\end{aligned}$$

When $\theta > tan^{-1}(\frac{k_i}{k_r})$, the divergent behavior of the resonant wave functions is regularized.

Complex scaling method

We want to calculate

- Narrow resonances in few-body systems
- Resonances in medium-mass region

$$\langle {}^{24}\mathrm{O} \otimes d^{(n)}_{3/2} | \, e^{-Ht} \, | {}^{24}\mathrm{O} \otimes d^{(n)}_{3/2} \rangle = \langle {}^{24}\mathrm{O} \otimes (d^{(n)}_{3/2})_{\mathrm{Resonance}} | \, e^{-Ht} \, | {}^{24}\mathrm{O} \otimes (d^{(n)}_{3/2})_{\mathrm{Resonance}} \rangle$$

$$\langle (d^{(n)}_{3/2})_{\mathrm{Resonance}} | \, e^{-Ht} \, | (d^{(n)}_{3/2})_{\mathrm{Resonance}} \rangle$$

Regularize the not square integrable part using exterior complex scaling.

$$O_{if} = \int_0^\infty u_f[r(\theta)] \hat{O} u_i[r(\theta)] dr$$

We need to solve

- Perform analytical continuation of lattice space interactions
- Test the convergence of lattice calculations
- Monte Carlo Sign problems
- Update the real and imaginary parts

Complex scaling method: Analytic continuation

- **Singularity in the potential:**

  HO basis expansion; N. Michel and M. Ploszajczak, Gamow Shell Model, Vol. 983 (Springer, 2021).

  Chebyshev polynomials; G. Kanwar, *et at.* arXiv:2304.03229.

- **Discontinuity in lattice space:**

  Laurent expansion; D. Agadjanov, *et at*. JHEP. 06 (2016) 043.

Continuum space:

numerical methods : four-point interpolation, Gauss-Legendre quadrature

N. Michel and M. Ploszajczak, Gamow Shell Model, Vol. 983 (Springer, 2021).

Lattice space:

uniform grid, step function, $g(x+dx) \approx g(x)$ on $[x,x+dx]$.

Analytic continuation

Contact term with Nearest-neighbor approximation:

Local smearing:

$$V_L(x) = \sum_{\hat{n}} c_{\hat{n}} \delta(x - \hat{n}a)$$

Transform to momentum space by FT and then perform the analytical continuation

$$\begin{aligned}
\langle p\prime| \, \delta(x - \hat{n}a) \, |p\rangle &= \int dx\prime dx \, \langle p\prime|x\prime\rangle \, \langle x\prime| \, \delta(x - \hat{n}a) \, |x\rangle \, \langle x|p\rangle \\
&= \int dx \delta(x - \hat{n}a) e^{-i(p-p\prime)x} \\
&= cos[(p - p\prime)\hat{n}a] \\
&\quad cos[(p - p\prime)\hat{n}a] \rightarrow cos[(U^{-1}(\theta)p - U^{-1}(\theta)p\prime)\hat{n}a]
\end{aligned}$$

Non-Local smearing:

$$\langle x| + s_{NL} \langle x + \hat{n}a| = [1 + \sum_n s_{NL} e^{ip\hat{n}a}] \langle x| = [1 + \sum_n s_{NL} cos(p\hat{n}a)] \langle x|$$

$$V(p,p\prime) = [1+s_{NL}cos(p\prime)][1+s_L cos(p-p\prime)]^2[c(p,p\prime)][1+s_{NL}cos(p)]e^{-\frac{(p^{2n}+p\prime^{2n})}{\Lambda^{2n}}}$$

1D 1-Body

Complex scaling method = Contour deformation

G. Hagen, et al.,, J. Phys. A 37, 8991 (2004)

Coordinate space → Momentum space

First, we need to check the effect of the discretization on analytical continuation in lattice space.

$$T\psi(p_\alpha) + \int_C dp_\beta V(p_\alpha, p_\beta)\psi(p_\beta) = E\psi(p_\alpha)$$

Lattice momentum mesh:

$$h_{\alpha,\beta} = T_{\alpha,\beta}\delta_{\alpha,\beta} + \Delta p_\beta V(p_\alpha, p_\beta)$$

Gauss-Legendre momentum mesh:

$$h_{\alpha,\beta} = T_{\alpha,\beta}\delta_{\alpha,\beta} + \sqrt{\omega_\alpha \omega_\beta} V(p_\alpha, p_\beta)$$

1D 1-Body

Complex scaling method = Contour deformation

G. Hagen, et al.,, J. Phys. A 37, 8991 (2004)

Coordinate space → Momentum space

$$\tan\delta = \frac{kj'_l(kR)\psi_{nl}(R) - j_l(kR)\psi'_{nl}(R)}{ky'_l(kR)\psi_{nl}(R) - y_l(kR)\psi'_{nl}(R)},$$

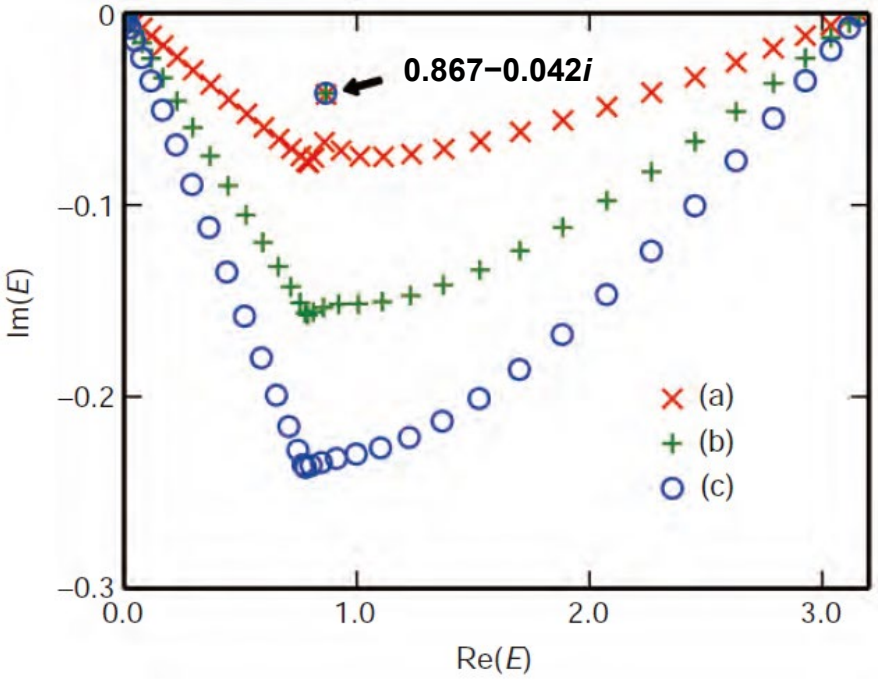

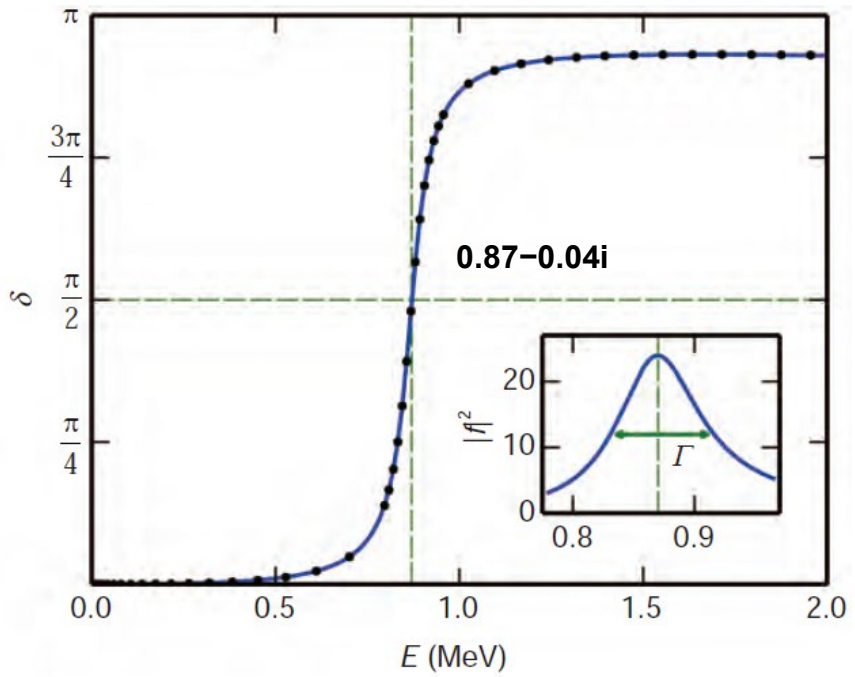

Contour deformation and Gauss-Legendre method works well in continuum space.

Benchmark using Gauss-Legendre methods with PBC

L	Shift	E_0(Lattice)	E_0(Gauss-Legendre)
12	0	-9.7982	-9.7982
	-0.5	(-9.7991, -0.00126)	(-9.7983, 0.00129)
	-1.0	(-9.8088, 0.02577)	(-9.7997, 0.04131)
24	0	-9.7982	-9.7982
	-0.5	(-9.7985, 0.00076)	(-9.7983, 0.00138)
	-1.0	(-9.8017, 0.03735)	(-9.7993, 0.04114)
360	0	-9.7982	-9.7982
	-0.5	(-9.7983, 0.00138)	(-9.7983, 0.00138)
	-1.0	(-9.7993, 0.04113)	(-9.7993, 0.04114)

Table 1: $H = T + V$, V is smeared contact term without regulator

1D 1-Body

With closed contour:

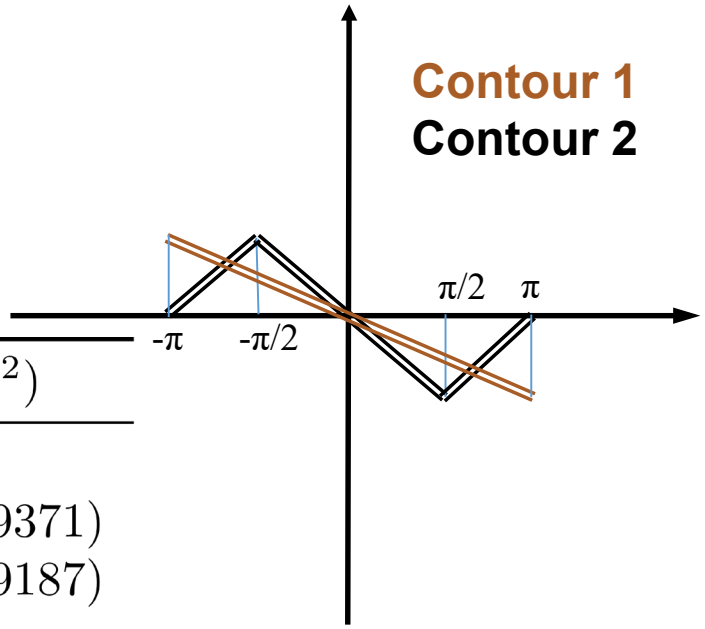

L	Shift	$E_0(\text{Lattice}^1)$	$E_0(\text{Lattice}^2)$
12	0	-9.7982	-9.7982
	-0.5	(-9.7991, -0.00126)	(-9.6947, -0.09371)
	-1.0	(-9.8088, 0.02577)	(-9.2614, -0.09187)
24	0	-9.7982	-9.7982
	-0.5	(-9.7985, 0.00076)	(-9.7729, -0.02387)
	-1.0	(-9.8017, 0.03735)	(-9.6696, -0.02546)
360	0	-9.7982	-9.7982
	-0.5	(-9.7983, 0.00138)	(-9.7981, -0.00011)
	-1.0	(-9.7993, 0.04113)	(-9.7977, -0.00012)

Table 1: $H = T + V$, V is smeared contact term without regulator

1D 1-Body

Regulator:

$$f_{NL}(p\prime, p) = e^{-b(\frac{p\prime}{\Lambda})^{2n}} e^{-b(\frac{p}{\Lambda})^{2n}}$$

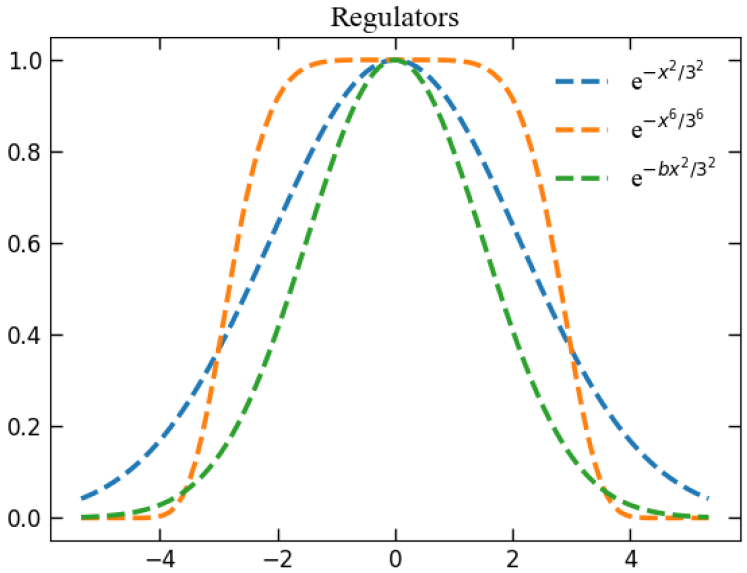

L	Shift	E_0(Lattice)	E_0(Gauss-Legendre)
12	0	-8.6239	-8.6237
	-0.5	(-8.6238, -0.00013)	(-8.6238, -0.00032)
	-1.0	(-8.6258, 0.00076)	(-8.6297, 0.00037)
24	0	-8.6239	-8.6239
	-0.5	(-8.6238, 0.00006)	(-8.6240, 0.00012)
	-1.0	(-8.6278, 0.00143)	(-8.6284, 0.00168)
360	0	-8.6239	-8.6239
	-0.5	(-8.6240, 0.00012)	(-8.6240, 0.00012)
	-1.0	(-8.6284, 0.00168)	(-8.6284, 0.00168)

Table 1: $H = T + V$, V is smeared contact term with regulator

1D 1-Body

L	Shift	$E_0(\alpha = 0.1)$	$E_0(\alpha = 1)$	$E_0(\alpha = 10)$	$E_1(\alpha = 10)$
12	0	-0.82882	-8.6239	-86.603	-8.6382
	-0.5	(-0.82882, -0.00001)	(-8.6238, -0.00013)	(-86.602, -0.00149)	(-8.6387, 0.00081)
	-1.0	(-0.82893, 0.00004)	(-8.6258, 0.00076)	(-86.623, 0.00860)	(-8.6580, 0.02229)
24	0	-0.82882	-8.6239	-86.603	-8.6382
	-0.5	(-0.82883, 0.00000)	(-8.6238, 0.00006)	(-86.603, 0.00065)	(-8.6382, 0.00004)
	-1.0	(-0.82905, 0.00004)	(-8.6278, 0.00143)	(-86.644, 0.01700)	(-8.6211, 0.00170)
360	0	-0.82882	-8.6239	-86.603	-8.6382
	-0.5	(-0.82883, 0.00001)	(-8.6240, 0.00012)	(-86.603, 0.00131)	(-8.6381, -0.00012)
	-1.0	(-0.82909, 0.00004)	(-8.6284, 0.00168)	(-86.650, 0.01999)	(-8.6112, 0.02097)

Table 1: $H = T + \alpha V$, V is smeared contact term with regulator

1D 1-Body

Resonance:

L	Shift	E_0(Lattice)	E_1(Lattice)	E_0(Gauss)	E_1(Gauss)
12	0	-1.0982		-1.0974	
	-0.5	(-1.0986, 0.00011)	(0.11434, -0.00448)	(-1.0979, -0.00078)	(0.12120, -0.01175)
	-1.0	(-1.0988, 0.00003)	(0.10754, -0.00418)	(-1.0990, -0.00174)	(0.10304, -0.01132)
24	0	-1.0983		-1.0983	
	-0.5	(-1.0985, 0.00002)	(0.11229, -0.00588)	(-1.0985, 0.00019)	(0.11162,-0.00520)
	-1.0	(-1.0985, 0.00010)	(0.10734, -0.00430)	(-1.0985, 0.00013)	(0.10723,-0.00436)
360	0	-1.0985		-1.0983	
	-0.5	(-1.0985, 0.00019)	(0.11243, -0.00627)	(-1.0985, 0.00019)	(0.11243,-0.00627)
	-1.0	(-1.0985, 0.00013)	(0.10718, -0.00444)	(-1.0985, 0.00013)	(0.10718, -0.00444)

Table 1: $H = T + V + V_p$, V_p is added to produce barrier.

$$V_p(p, p\prime) = -c_p \cdot (p - p\prime)^2 e^{-0.7\cdot[(p-p\prime)^2 + M_\pi^2]} / [(p - p\prime)^2 + M_\pi^2]$$

$$c_p = 1.1; M_\pi = 139/150$$

Convergence of the calculations:

$$V(p\prime_1, p\prime_2; p_1, p_2) = [1 + s_{NL}cos(p\prime_1)][1 + s_{NL}cos(p\prime_2)][1 + 2s_Lcos(p_1 - p\prime_1)]$$
$$*[1 + 2s_Lcos(p_2 - p\prime_2)][c(p, p\prime)][1 + 2s_{NL}cos(p_2)]$$
$$*[1 + s_{NL}cos(p_1)]e^{-\frac{e_{fac}(p_1^{2n} + p\prime_1^{2n} + p_2^{2n} + p\prime_2^{2n})}{\Lambda^{2n}}}$$

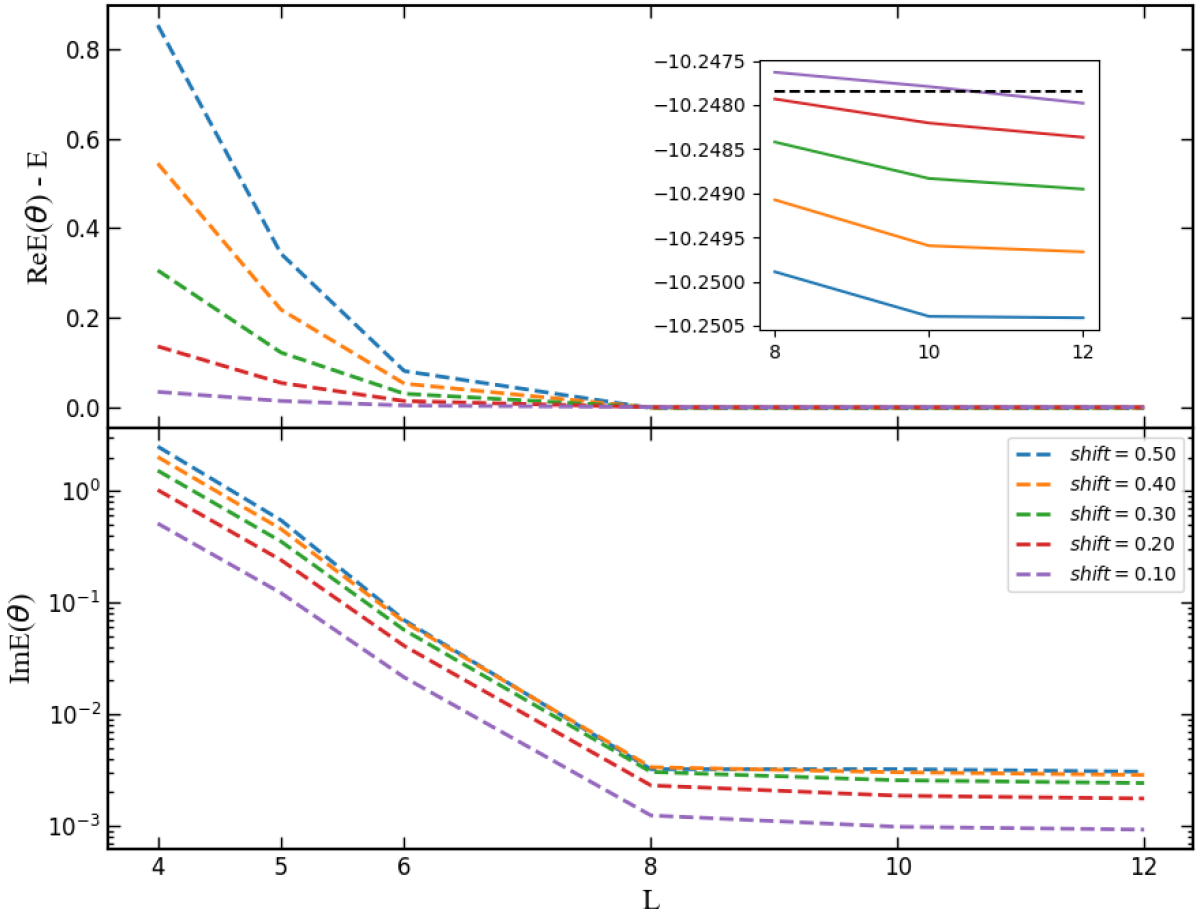

NLEFT calculations of proton-rich nuclei

- **Experimental and theoretical study on ^{22}Si**
- **NLEFT calculated g.s. of ^{22}Si, ^{20}Mg**
- **2^+ states of ^{22}Si, ^{20}Mg, ^{18}Mg and ^{16}Ne & shell closure**

NLEFT calculations of proton-rich nuclei

^{22}Si	method	S_{2p}	notes
	EXP[1]	645(100) keV	weakly bound, indirect experimental measurement **M. Babo, Thesis, Université de Caen Normandie (2016)**
	EXP[2]	-108(125) keV	weakly unbound, indirect experimental measurement **X.X. Xu, et al., PLB 766, 312 (2017)**
	MBPT	-120 keV	2-p emission candidates, chiral NN+3N, $sdp_{3/2}f_{7/2}$ **J.D. Holt, et al., PRL 110, 022502 (2013)**
	IMSRG	-382 keV$\sim$ -558 keV	weakly unbound, EM1.8/2.0, different valence spaces **S.R. Stroberg, et al., PRL 126, 022501 (2017)**
	GSM	674 keV	weakly bound, chiral NN+3N, $sdp_{3/2}f_{7/2}$ **S. Zhang, et al., PLB 827, 136958 (2022)**

Table 1: Current status of experimental and theoretical study on ^{22}Si

NLEFT calculations of proton-rich nuclei

Lanzhou CSR

The High-Precision Measurement Facility for Short-lived Nuclear Masses recently measured ^{22}Si.

M. Zhang, *et al.*, *Eur. Phys. J. A* **59**, 27 (2023).

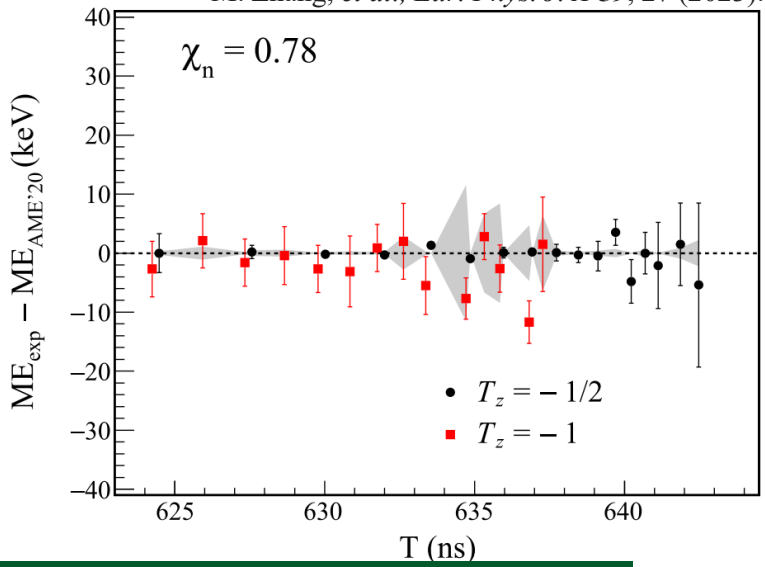

FRIB

FRIB Scientific User Portal

Approved Experiments | Public Experiment List

The following is a list of approved experiments at FRIB. Click on a column header to sort by that column.

Show 25 entries Search: 22Si

Experiment Number	Contact Spokesperson	Co-Spokespersons	Title	Beam on Target Hours Approved	Beam Tuning Hours	Date Completed
21006	Charity, Robert		Is 22Si a doubly-magic nucleus?	160	24	

NLEFT calculations of proton-rich nuclei

Method:

NLEFT with chiral force at N^{3}LO using wave function matching

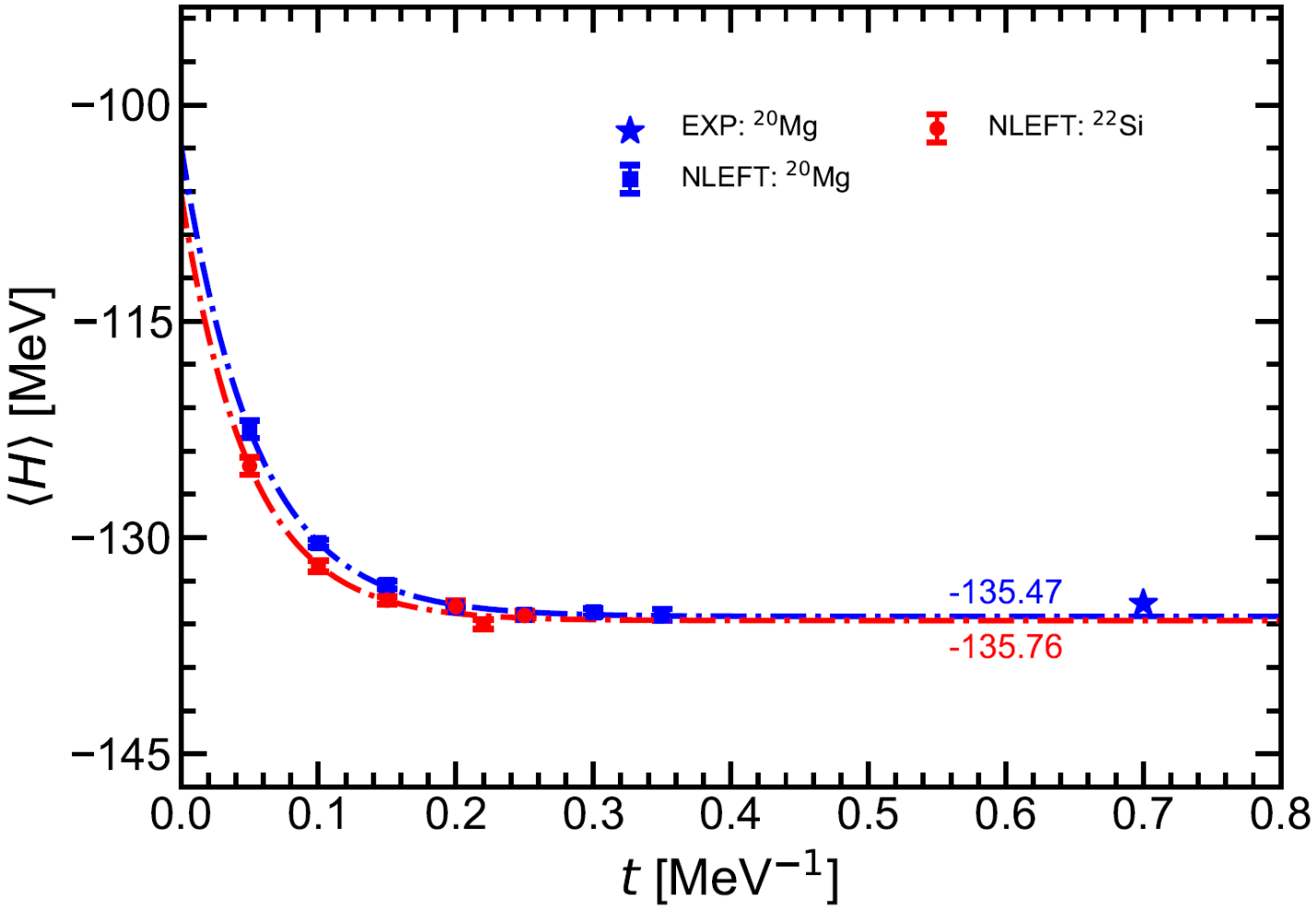

NLEFT calculations of proton-rich nuclei

Y. Jin, et al., Phys. Rev. Lett. 127, 262502 (2021)

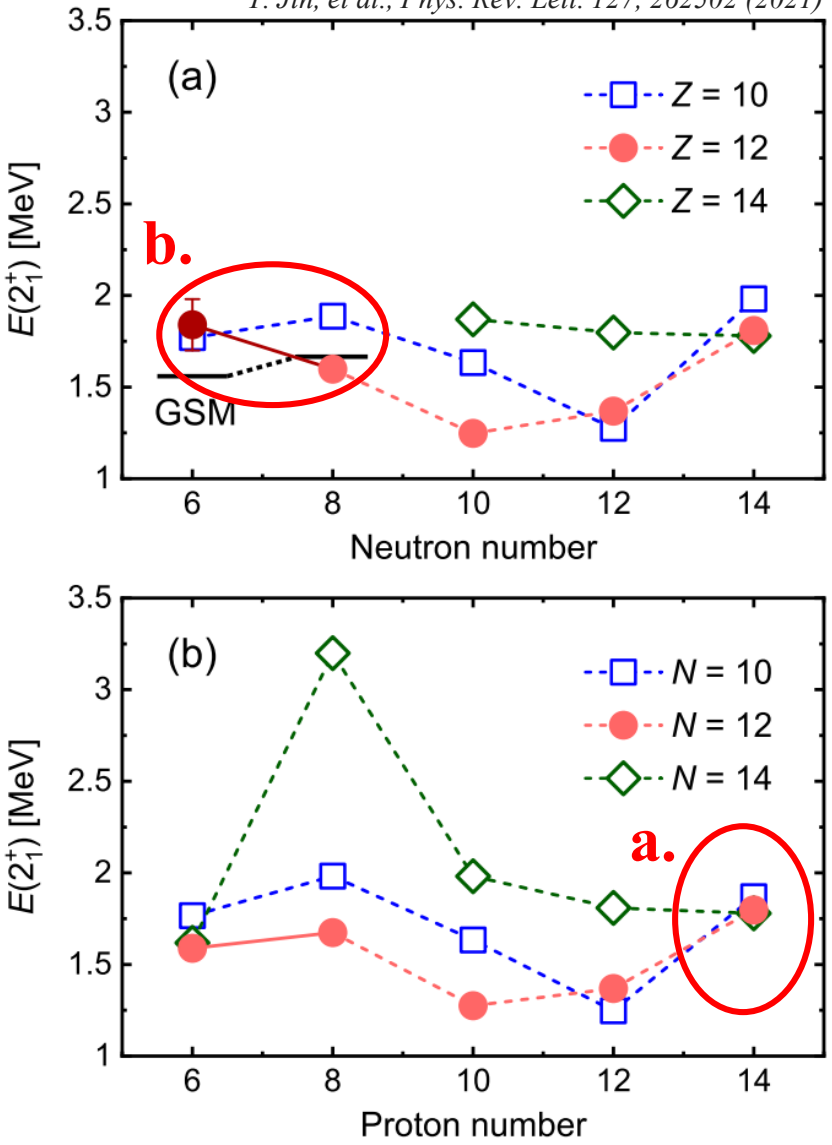

a. **Z = 14 is a magic number when N = 10 and N = 12**

b. **Shell weakening of N = 8 at Z = 12**

c. **4^+ significantly higher than theoretical calculations**

J. S. Randhawa , et al., Phys. Rev. C 99, 021301(R) (2019)

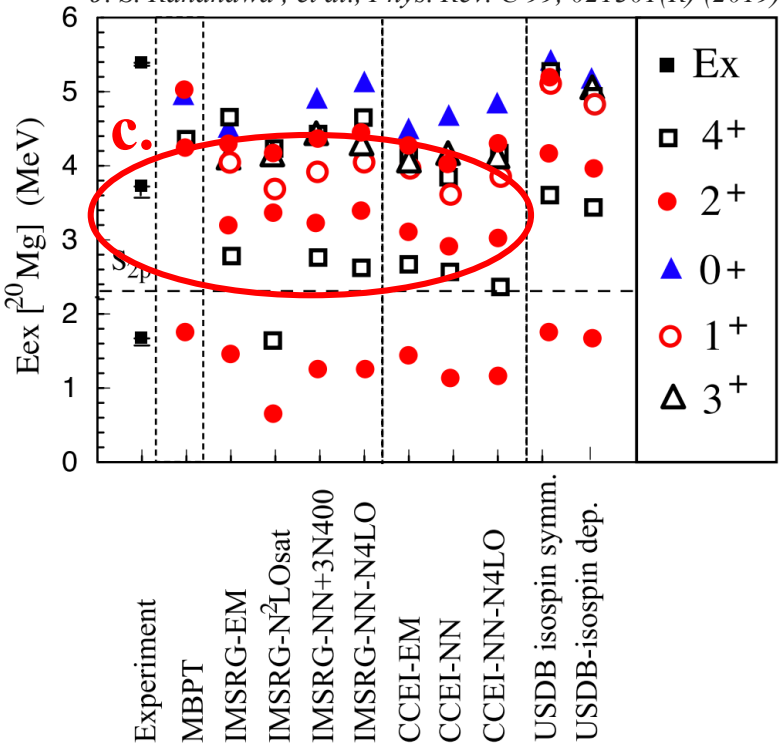

NLEFT calculations of proton-rich nuclei

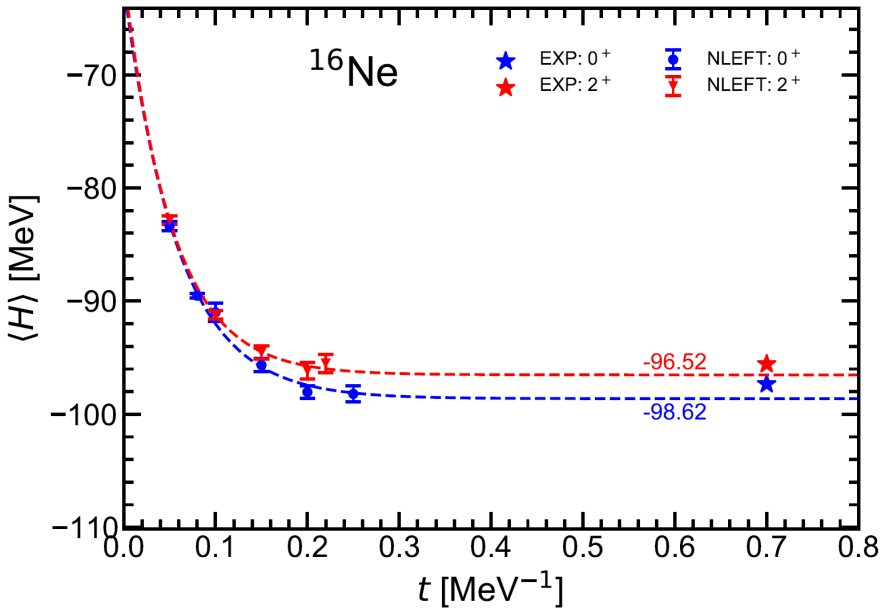

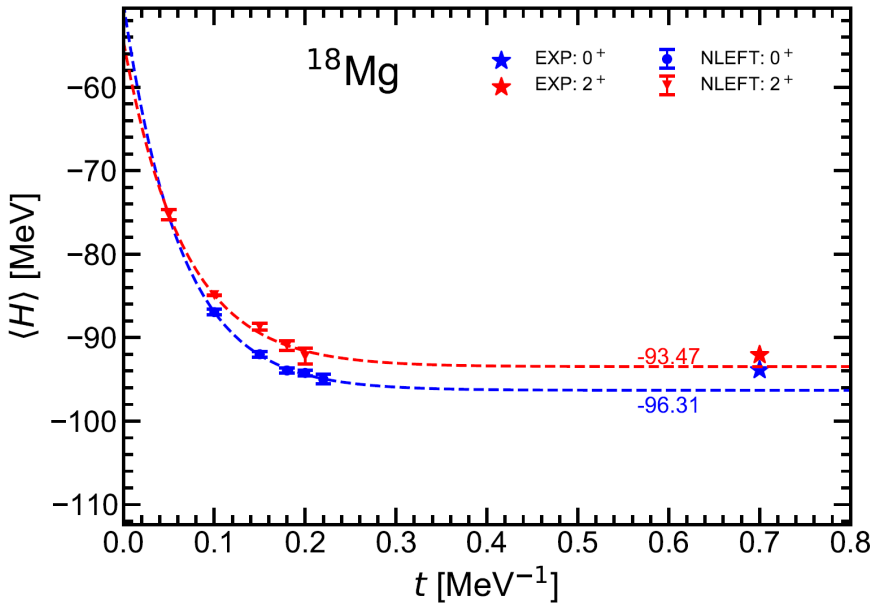

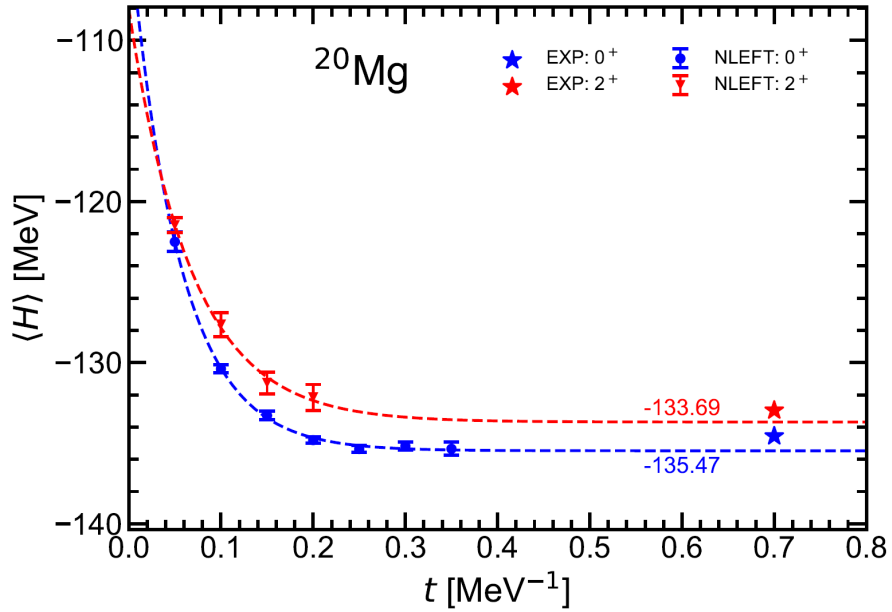

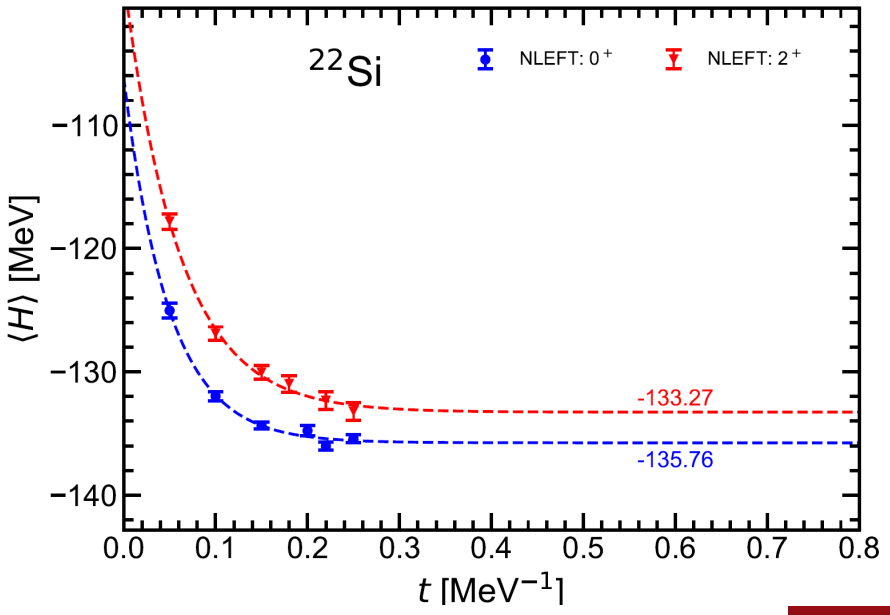

NLEFT calculations of proton-rich nuclei

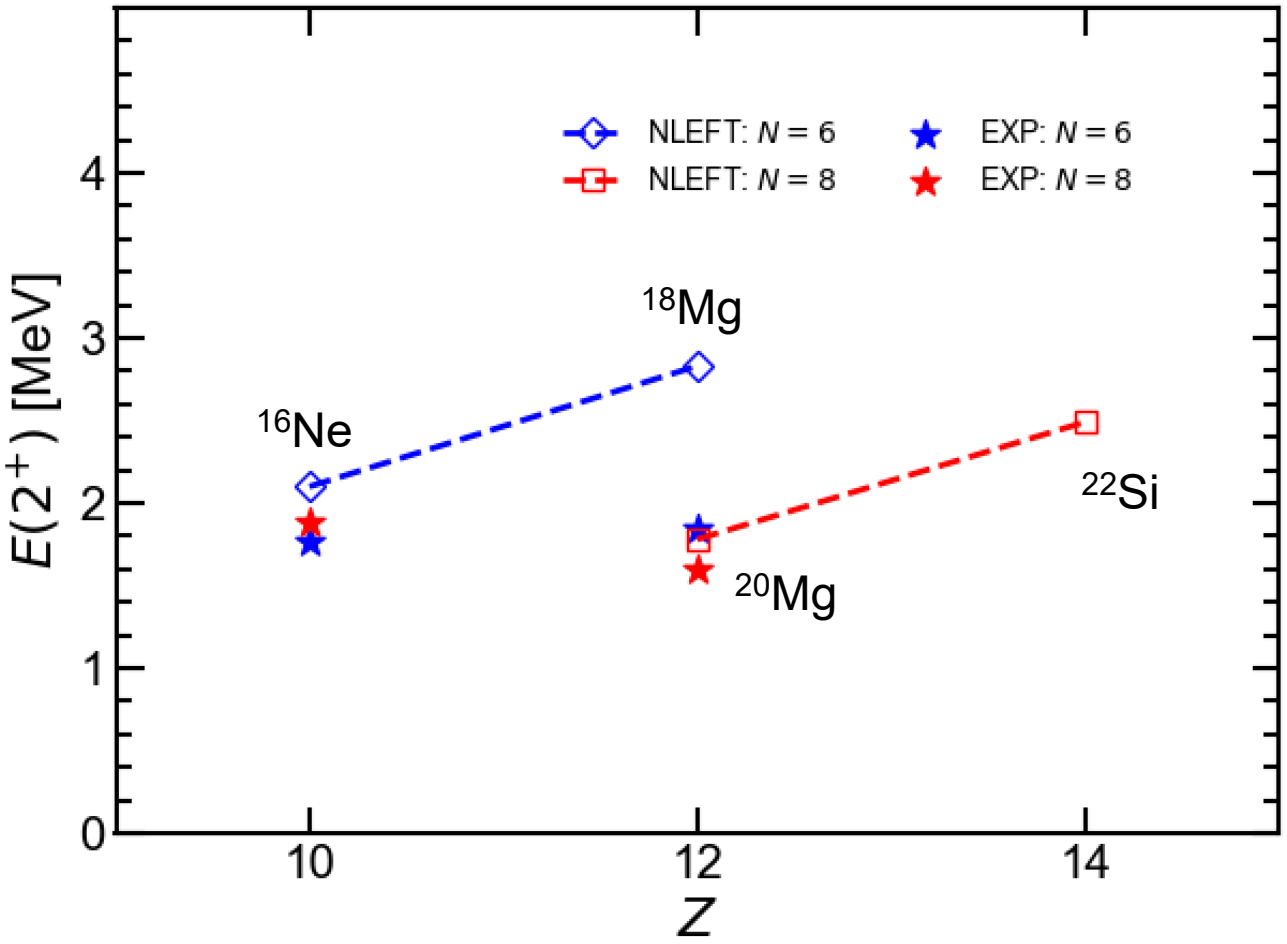

The 2^+ state of ^{22}Si is compared with that of ^{20}Mg and ^{18}Ne to account for the Z=14 shell.

The 2^+ state of ^{18}Mg is higher than that in ^{20}Mg.

Summary & perspective

- Complex scaling in NLEFT
  - Complex scaling method
  - Exact solutions in 3D 2-body systems
- NLEFT calculations of proton-rich nuclei
  - Calculated g.s. of ^{22}Si, ^{20}Mg
  - 2^+ states & shell closure
- Further developments
  - Exact solutions in 3-body systems, complex scaling in Monte Carlo simulations, …
  - More excited states, radii, density distributions for *p*-rich nuclei

Thank you!

G. H. Booth, *et al*., Nature 2013,493, 365-370

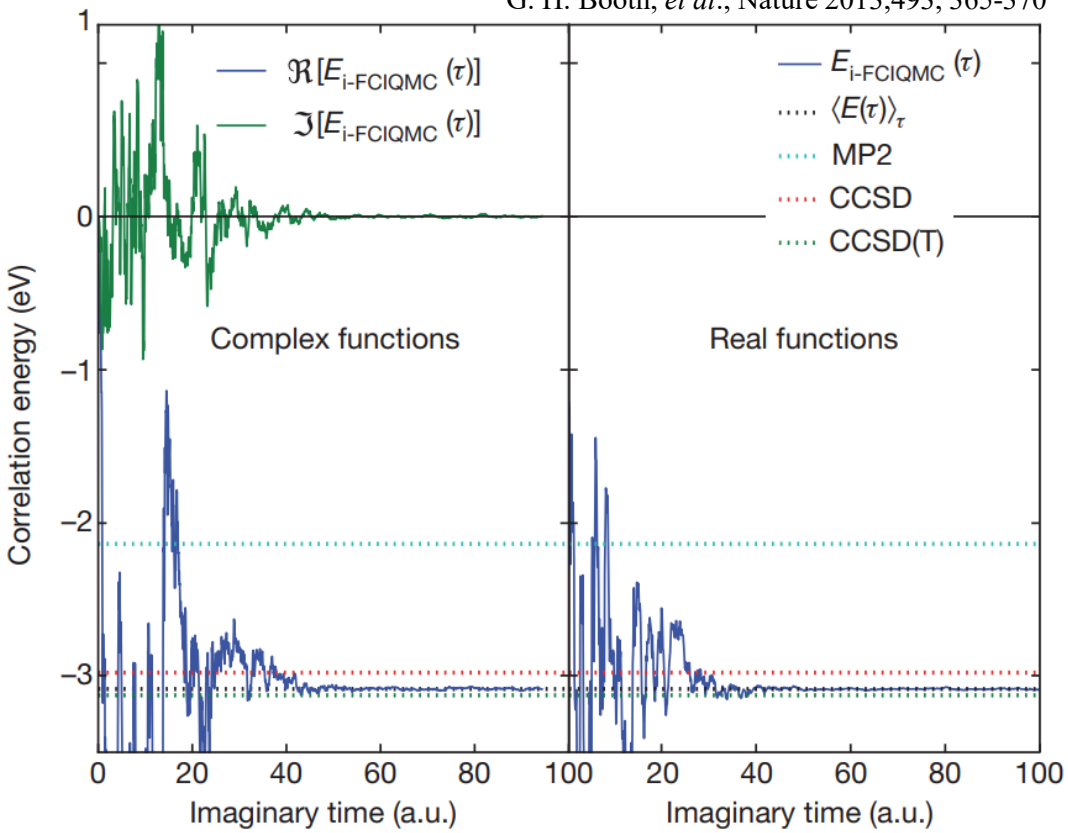

Figure 2 | Comparison of real and complex i-FCIQMC dynamics for the correlation energy of LiH. A $2 \times 2 \times 2$ Γ-centred k-point mesh with 16 electrons, and 40 correlated Hartree–Fock orbitals was employed, at a primitive rock-salt unit cell volume of 17.03 Å^3. Converged energies for 30 million walkers between the two bases agree within small stochastic error bars. The additional overhead for the complex dynamic means that the cost was ~5 times that of the real dynamic to converge to equivalent error bars. Also included are MP2, CCSD and CCSD(T) results for comparison. $\langle E(\tau)\rangle_\tau$ is an imaginary-time average of the projected energy $E(\tau)$, taken after a period of equilibration.

Sign problems

$$e^{-S[s]} \qquad e^{-S[s,\theta]} \qquad e^{-S[s,\pi,\cdots]} \qquad e^{-S[s,\pi,\theta,\cdots]}$$

$$\tilde{s} = s + i\lambda$$

$$s^2 - \lambda^2 + 2is\lambda + i(s + i\lambda)$$

$$\int ds e^{s^2+is} = \int d\tilde{s} e^{\tilde{s}^2+i\tilde{s}}$$

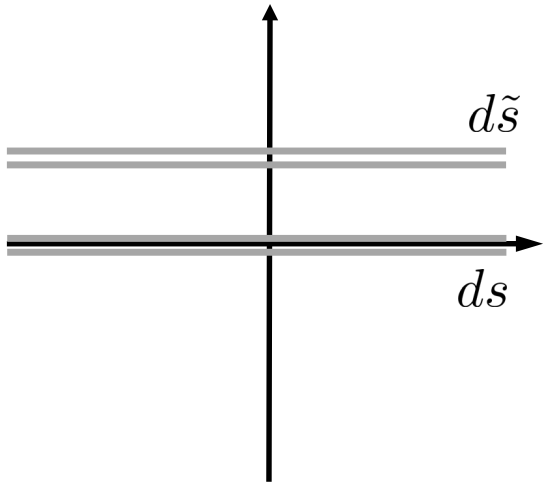

$$s(x,t) \qquad \tilde{s}(x,t) = s(x,t) + i\lambda(x,t)$$

$$\pi(x,t) \qquad \tilde{\pi}(x,t) = \pi(x,t) + i\mu(x,t)$$

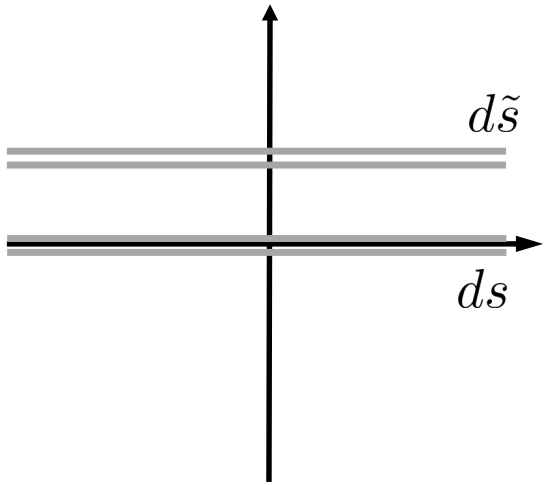

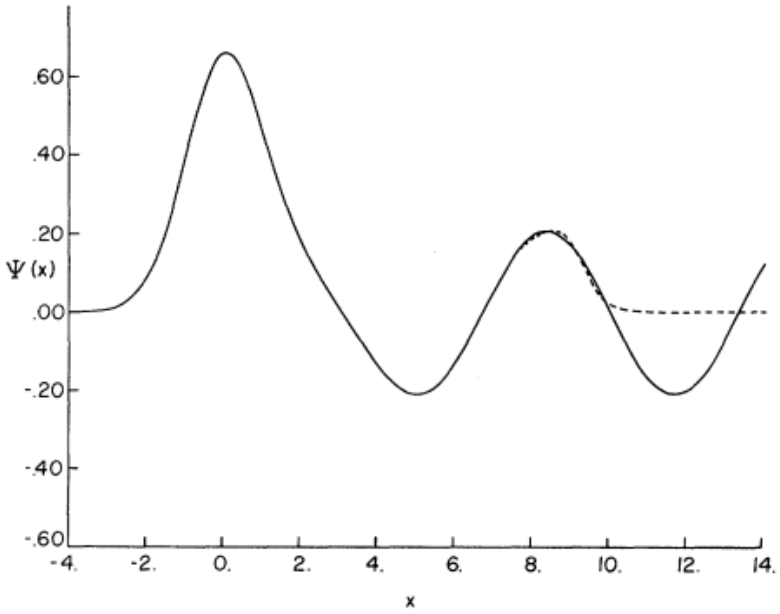

A. U. Hazi and H. S. Taylor, Phys. Rev. A 1, 1109–1120 (1970).